JPEDAV (2007) 28:342–354
DOI: 10.1007/s11669-007-9095-9
1547-7037 ©ASM International

Critical Evaluation and Thermodynamic Optimization of the Binary Systems in the Mg-Ce-Mn-Y System

Youn-Bae Kang, Arthur D. Pelton, Patrice Chartrand, Philip Spencer and Carlton D. Fuerst

(Submitted August 2, 2006; in revised form October 4, 2006)

Critical evaluation and thermodynamic optimization have been carried out for the Mg-Ce, Mg-Mn, Mg-Y, Ce-Mn, Ce-Y, and Mn-Y binary systems. All phase diagrams and thermodynamic data such as enthalpies of mixing, heats of formation, etc., were considered to obtain one set of model parameters of the Gibbs energies of all phases, which can reproduce the experimental data within experimental error limits. For the liquid alloys, the Modified Quasi-chemical Model in the pair approximation was used to treat short-range-ordering.

Keywords magnesium alloys, Mg-Ce-Mn-Y system, Modified Quasi-chemical Model, thermodynamic databases, thermodynamic modeling

1. Introduction

Although magnesium-based materials have a long history of important commercial applications, including automotive, there remains much to be learned about the basic properties of the metal and its alloys. With the recent renewed interest in lightweight wrought materials, including both sheet and tube applications, there has been an increased focus on developing a better understanding of novel magnesium alloy systems, including those that incorporate additions of such elements as Ce, Y, and Mn. These alloy systems, along with other potential candidates, are being actively pursued as possible routes to develop magnesium materials with improved ductility, or even practical room-temperature formability.

As part of a broader research project to develop a comprehensive thermodynamic database for Mg alloys with 25 potential alloying elements, we have prepared a critically evaluated and optimized database for the Mg-Ce-Mn-Y system. The present article reports on our evaluation/optimizations of the six binary subsystems. In a subsequent article,[1] we report on optimizations for the ternary subsystems.

The Ce-Mn and Ce-Y systems are evaluated/optimized for the first time. The other four binary systems have been assessed previously. However, we have reassessed these systems for the following reasons. (a) Some new experimental data have become available since the previous assessments were published. (b) In certain areas the agreement between the previous optimizations and the experimental data was not sufficiently precise, particularly as regards solubilities in the Mg(HCP-A3) phase, which are of prime importance to the development of new alloys. (c) The liquid Mg-Ce and Mg-Y phases show clear evidence of short-range-ordering (SRO). In the present assessment, this is taken into account through use of the Modified Quasi-chemical Model (MQM). This provides better representations of the partial properties of solutes in Mg-rich alloys and better estimations of the properties of ternary and higher-order liquid phases. (d) In the present optimizations the Laves phases are modeled using the compound energy formalism (CEF), thereby permitting their incorporation into ternary and higher-order solutions. (e) The previously assessed critical temperature of the Mg-Mn liquid-liquid miscibility gap was much too high, leading to the prediction of a large miscibility gap in the Mg-Mn-Y ternary system in disagreement with observations.

Youn-Bae Kang, Arthur D. Pelton, and **Patrice Chartrand,** CRCT (Centre de Recherche en Calcul Thermochimique), Département de génie chimique, École Polytechnique, succ. Centre-ville, C.P. 6079 Montréal, QC, Canada H3C 3A7; **Philip Spencer,** The Spencer Group, 9551, Kingtown Rd., Trumansburg, NY 14886, USA; **Carlton D. Fuerst,** General Motors, MC 480-106-224, 30500 Mound Rd., Warren, MI 48090-9055, USA; Contact e-mail: apelton@polymtl.ca

2. Thermodynamic Models and Parameters

All calculations and optimizations in the present study were performed with the FactSage thermochemical software.[2,3]

The Gibbs energies of all phases of pure Mg, Mn, and Ce were taken from Dinsdale,[4] except for the HCP-A3 and the DHCP phases of Ce as are discussed in sections 3.4 and 3.5. The Gibbs energies of all phases of pure Y were taken from Dinsdale.[5] A list of all the binary phases in the six binary systems considered in the present study is given in Table 1. The following is a brief outline of the models used for these phases.

2.1 Liquid Solution

The Modified Quasi-chemical Model (MQM) in the pair approximation[6] was used to model the liquid alloys. This model, which takes SRO into account, has been used

Table 1 All binary phases in the Mg-Ce-Mn-Y system considered in the present study

Phase	Strukturbericht	Prototype	Pearson Symbol	Space Group	Model[(a)]	Note
Liquid	...	...	...	...	MQM	
FCC	*A*1	Cu	*cF*4	$Fm\bar{3}m$	CEF	Ce, Mn are stable phases.
BCC	*A*2	W	*cI*2	$Im\bar{3}m$	CEF	Ce, Mn, Y are stable phases.
HCP	*A*3	Mg	*hP*2	$P6_3/mmc$	CEF	Mg, Y are stable phases.
DHCP	*A*3′	α-La	*hP*4	$P6_3/mmc$	CEF	Ce is a stable phase.
$Mg_{24}Y_5$	*A*12	α-Mn	*cI*58	$I\bar{4}3m$	CEF	
Laves-C14	*C*14	$MgZn_2$	*hP*12	$P6_3/mmc$	CEF	Mg_2Y is a stable phase.
Laves-C15	*C*15	Cu_2Mg	*cF*24	$Fd\bar{3}m$	CEF	$CeMg_2$, Mn_2Y are stable phases.
BCC-B2	*B*2	CsCl	c*P*2	*Pm*3*m*	CEF	MgY, CeMg are stable phases.
$CeMg_3$	$D0_3$	$AlFe_3$	*cF*16	$Fm\bar{3}m$	CEF	Limited solubility of Y[(b)]
$Mn_{23}Y_6$	$D8_a$	$Mn_{23}Th_6$	*cF*116	$Fm\bar{3}m$	CEF	Limited solubility of Mg and Ce[(b)]
$CeMg_{12}$	$D2_b$	$Mn_{12}Th$	*tI*26	*I*4/*mmm*	ST	
CBCC(Mn)	*A*12	α-Mn	*c*58	$I\bar{4}3m$	ST	
CUB(Mn)	*A*13	β-Mn	*cP*20	$P4_132$	ST	
$Mn_{12}Y$	$D2_h$	$Mn_{12}Th$	*tI*26	*I*4/*mmm*	ST	
Ce_5Mg_{41}	...	Ce_5Mg_{41}	*tI*92	*I*4/*m*	ST	
Ce_2Mg_{17}	...	$Ni_{17}Th_2$	*hP*38	$P6_3/mmc$	ST	

(a) MQM, Modified Quasi-chemical Model; ST, stoichiometric compound; CEF, compound energy formalism; (b) Ref 1

extensively for molten salts,[7-9] slags,[10] and sulfides.[11-13] All details of the model and notation have been described previously,[6,12] and only a brief summary is given here.

In the MQM in the pair approximation, the following pair exchange reaction between atoms A and B on neighboring lattice sites is considered:

$$(A-A)+(B-B)=2(A-B); \qquad \Delta g_{AB} \qquad \text{(Eq 1)}$$

where (i–j) represents a first-nearest-neighbor pair. The nonconfigurational Gibbs energy change for the formation of 2 moles of (A–B) pairs is Δg_{AB}.

Let n_A and n_B be the number of moles of A and B, n_{ij} be the number of moles of (i–j) pairs, and Z_A and Z_B be the coordination numbers of A and B. The pair fractions, mole fractions, and "coordination-equivalent" fractions are also defined respectively as:

$$X_{ij}=n_{ij}/(n_{AA}+n_{BB}+n_{AB}) \qquad \text{(Eq 2)}$$

$$X_A=n_A/(n_A+n_B)=1-X_B \qquad \text{(Eq 3)}$$

$$Y_A=\frac{Z_An_A}{(Z_An_A+Z_Bn_B)}=\frac{Z_AX_A}{(Z_AX_A+Z_BX_B)}=1-Y_B \qquad \text{(Eq 4)}$$

The Gibbs energy of the solution is given by:

$$G=\left(n_Ag_A^\circ+n_Bg_B^\circ\right)-T\Delta S^{\text{config}}+(n_{AB}/2)\Delta g_{AB} \qquad \text{(Eq 5)}$$

where g_A° and g_B° are the molar Gibbs energies of the pure components, and ΔS^{config} is the configurational entropy of mixing given by randomly distributing the (A–A), (B–B), and (A–B) pairs in the one-dimensional Ising approximation:[6]

$$\Delta S^{\text{config}}=-\text{R}(n_A\ln X_A+n_B\ln X_B) -\text{R}\left[n_{AA}\ln\left(\frac{X_{AA}}{Y_A^2}\right)+n_{BB}\ln\left(\frac{X_{BB}}{Y_B^2}\right)+n_{AB}\ln\left(\frac{X_{AB}}{2Y_AY_B}\right)\right] \qquad \text{(Eq 6)}$$

Δg_{AB} is expanded in terms of the pair fractions:

$$\Delta g_{AB}=\Delta g_{AB}^\circ+\sum_{i\geq1}g_{AB}^{i0}X_{AA}^i+\sum_{j\geq1}g_{AB}^{0j}X_{BB}^j \qquad \text{(Eq 7)}$$

where Δg_{AB}°, g_{AB}^{i0}, and g_{AB}^{0j} are the parameters of the model that can be functions of temperature.

The equilibrium pair distribution is calculated by setting

$$(\partial G/\partial n_{AB})_{n_A,n_B}=0 \qquad \text{(Eq 8)}$$

This gives the "equilibrium constant" for the "quasi-chemical reaction" of (Eq 1):

$$\frac{X_{AB}^2}{X_{AA}X_{BB}}=4\exp\left(-\frac{\Delta g_{AB}}{RT}\right) \qquad \text{(Eq 9)}$$

As Δg_{AB} becomes progressively more negative, the reaction (Eq 1) is shifted progressively to the right, and the calculated enthalpy and configurational entropy of mixing assume, respectively, the negative "V" and "m" shapes characteristic of SRO as in the Mg-Ce system discussed in section 3.5.

The composition of maximum SRO is determined by the ratio of the coordination numbers Z_B/Z_A. For example, to set this composition at $X_{\text{Mg}}=3/4$, (corresponding to the composition $CeMg_3$) in the Mg-Ce system, we set the ratio $Z_{\text{Mg}}/Z_{\text{Ce}}=1/3$. Although the model is sensitive to the ratio of the coordination numbers, it is less sensitive to their absolute values. The use of the one-dimensional Ising model

in (Eq 6) introduces a mathematical approximation into the model that we have found, by experience, can be partially compensated by selecting values of Z_B and Z_A which are smaller than the actual values. For example, for the Mg-Ce system we have chosen $Z_{Mg} = 2$ and $Z_{Ce} = 6$.

When Δg_{AB} is small, it can be shown[6] that the configurational entropy of mixing is approximately equal to the random-mixing Bragg-Williams value and that the excess Gibbs energy becomes approximately:

$$G^E \cong (Z_A n_A + Z_B n_B) Y_A Y_B \Delta g_{AB}/2 \quad \text{(Eq 10)}$$

If $Z_A = Z_B$, then $Y_A = X_A$ and $Y_B = X_B$. If, further, Δg_{AB} is constant, (Eq 10) becomes a simple regular solution expression with a minimum (or maximum depending on the sign of Δg_{AB}) at $X_A = X_B = 1/2$. Suppose now that the experimental data indicate that the extremum in G^E occurs, for example, close to $X_B = 1/4$ rather than at $X_B = 1/2$. We could shift the extremum in the usual way by making Δg_{AB} a linear function of composition (subregular model). However, this can often result in poor fitting of the partial properties at compositions near $X_B = 1.0$. For example, in the case where $G^E < 0$, if we wish to shift the minimum to $X_B = 1/4$ by using the subregular model, then we must set $G^E = a + bX_B$ where $a < 0$ and $b > 0$. This causes the partial excess Gibbs energy of component B to increase, and even to become positive, at high values of X_B.

Another way to shift the composition of the minimum without this undesirable side effect is to keep Δg_{AB} constant and to choose Z_A and Z_B such that $Z_B/Z_A = 3$. Examples are given for the Mn-Y and Ce-Mn systems in sections 3.1 and 3.3.

2.2 Solid Solutions

All solid solutions were modeled using the well-known Compound Energy Formalism (CEF).[14] For example, the Laves phase $(Mg,Y)_2^a\,[Mg,Y]_1^b$ has two sublattices, the a and b lattices, with Mg and Y on both lattices. Its Gibbs energy in the CEF is given by

$$\begin{aligned} G = {} & y^a_{Mg} y^b_{Mg} G_{Mg:Mg} + y^a_{Mg} y^b G_{Mg:Y} + y^a_Y y^b_{Mg} G_{Y:Mg} + y^a_Y y^b_Y G_{Y:Y} \\ & + 2RT\left(y^a_{Mg} \ln y^a_{Mg} + y^a_Y \ln y^a_Y\right) + RT\left(y^b_{Mg} \ln y^b_{Mg} + y^b_Y \ln y^b_Y\right) \\ & + \sum_{i,j,k} y^a_i y^a_j y^b_k L_{ij:k} + \sum_{i,j,k} y^a_k y^b_i y^b_j L_{k:ij} \end{aligned} \quad \text{(Eq 11)}$$

where y^a_i, y^b_i are site fractions of component i on each sublattice, and $G_{i:j}$ is the Gibbs energy of end member $(i)_2^a\,[j]_1^b$. A Gibbs energy $G_{i:j}$ is required for every possible end member pair. $L_{ij:k}$ and $L_{k:ij}$ are interaction parameters between components i and j on one sublattice when the other sublattice is occupied only by k.

Some of the Laves phases observed in the present binary systems, Mg_2Ce and Mn_2Y, show only negligible deviation from stoichiometry. Hence, only $G_{Mg:Ce}$ and $G_{Mn:Y}$ are sufficient to describe these phases in the binary systems. That is, in the binary systems they can be described as stoichiometric compounds. However, these binary Laves phases form solid solutions in ternary and higher-order systems which we are modeling as part of our larger study. Hence, all possible $G_{i:j}$ values must be defined. For example, the Laves-C15 phase in the Mg-Ce-Mn-Y system was modeled with 16 end members. Among these end members, Mg_2Ce and Mn_2Y are stable and almost stoichiometric compounds in the Mg-Ce and Mn-Y binary systems, respectively. Hence, $G_{Mg:Ce}$ and $G_{Mn:Y}$ are directly taken from the Gibbs energies of the corresponding compounds. Gibbs energies of several other end members were optimized from the known solid solubilities in binary, ternary, or higher-order systems. For example, $G_{Mg:Y}$ in the Laves-C15 phase was optimized to reproduce the solubility of Mg in Mn_2Y.[1] The Gibbs energies of the remaining end members were arbitrarily set to high positive values so that unknown solid solubilities are calculated to be negligible.

3. Critical Evaluation and Thermodynamic Optimization of Binary Systems

The optimized model parameters for all phases as obtained in the present study are listed in Table 2.

3.1 The Mn-Y System

This system was extensively reviewed by Palenzona and Cirafici[15] and was thermodynamically optimized by Flandorfer et al.[16] and Gröbner et al.[17]

The earlier optimization[16] was based mainly on DTA data from Myklebust and Daane.[18] Clearly, phase diagram data alone are not sufficient for a complete thermodynamic optimization. A later investigation by Pisch et al.[19] of the enthalpies of formation of intermetallic compounds in the Mn-Y system by aluminum drop solution calorimetry showed that the optimized enthalpies of formation of the binary intermetallic compounds[16] were too negative. Hence the optimized Gibbs energy of liquid Mn-Y alloys was also too negative. Gröbner et al.[17] reoptimized the system using the newly determined enthalpies of formation.[19] However, the enthalpy of mixing measured by isoperibol calorimetry[20] could not be well reproduced as can be seen in Fig. 1 and 2. The minimum in the enthalpy of mixing curve near $X_Y = 0.25$ suggests the use of the MQM with $Z^{Mn}_{MnY}/Z^{Y}_{MnY} = 1/3$.

Figure 3 shows the phase diagram optimized in the present study along with the DTA measurements of Myklebust and Daane.[18] Agreement between calculation and experiment is good except for the two experimental points on the liquidus of Y(HCP). Since it has been reported that Mn does not dissolve in Y(HCP),[16] these two measured points are almost certainly in error because they violate the limiting liquidus slope rule.[21]

Figure 4 shows the enthalpy of formation of intermetallic compounds. Calorimetrically determined data by Pisch et al.[19] are compared with calculations from the present optimization and from those of Flandorfer et al.[16] and Gröbner et al.[17] As seen in the figure, the measured enthalpy of formation of Mn_2Y is higher than the average of

Table 2 Optimized model parameters of all binary phases in the Mg-Ce-Mn-Y system (J/mole)

Liquid Alloy

Coordination Numbers[a]				Gibbs energies of pair exchange reactions
i	j	Z^i_{ij}	Z^j_{ij}	
Ce	Mg	6	2	$\Delta g_{CeMg} = -15{,}899.2 + 7.43T - 8{,}368X_{CeCe} + (-9{,}623.2 + 2.51T)X_{MgMg}$
Ce	Mn	6	3	$\Delta g_{CeMn} = 5020.8 - 1.26T + (-627.6 + 2.1T)X_{CeCe} + 836.8X_{MnMn}$
Ce	Y	6	6	$\Delta g_{CeY} = 697.33$
Mg	Mn	6	6	$\Delta g_{MgMn} = 14{,}644 + (-7{,}471.91 + 3.49T)X_{MgMg}$
Mg	Y	3	6	$\Delta g_{MgY} = -12{,}761.2 + 3.77T + (-8368 + 6.28T)X^2_{MgMg} + 2092X^2_{YY}$
Mn	Y	2	6	$\Delta g_{MnY} = -3356.4 - 0.50T - 1255.2X^2_{MnMn} + (-418.4 - 3.35T)X^2_{YY}$

Laves-C14 ($MgZn_2$-type): (Ce, Mg, Mn, Y)$_2$[Ce, Mg, Mn, Y]

G(Ce:Ce) = 3G(Ce,FCC-A1) + 30,000
G(Ce:Mg) = 2G(Ce,FCC-A1) + G(Mg,HCP-A3) + 41,840
G(Ce:Mn) = 2G(Ce,FCC-A1) + G(Mn,CBCC-A12) + 41,840
G(Ce:Y) = 2G(Ce,FCC-A1) + G(Y,HCP-A3) + 41,840
G(Mg:Ce) = 2G(Mg,HCP-A3) + G(Ce,FCC-A1) − 43,264.73 + 10.35T
G(Mg:Mg) = 3G(Mg,HCP-A3) + 15,000[b]
G(Mg:Mn) = 2G(Mg,HCP-A3) + G(Mn,CBCC-A12) + 83,680
G(Mg:Y) = 2G(Mg,HCP-A3) + G(Y,HCP-A3) − 37,548.96 + 6.6T
G(Mn:Ce) = 2G(Mn,CBCC-A12) + G(Ce,FCC-A1) + 41,840
G(Mn:Mg) = 2G(Mn,CBCC-A12) + G(Mg,HCP-A3) + 83,6804
G(Mn:Mn) = 3G(Mn,CBCC-A12) + 3000[c]
G(Mn:Y) = 2G(Mn,CBCC-A12) + G(Y,HCP-A3) + 14,983.568 + 12.57T
G(Y:Ce) = 2G(Y,HCP-A3) + G(Ce,FCC-A1) + 41,840
G(Y:Mg) = 2G(Y,HCP-A3) + G(Mg,HCP-A3) + 67,548.96 − 6.6T
G(Y:Mn) = 2G(Y,HCP-A3) + G(Mn,CBCC-A12) + 23,936 − 12.57T
G(Y:Y) = 3G(Y,HCP-A3) + 15,000[d]
$L_{Mg,Y:Mg} = L_{Mg,Y:Y}$ = 21,000[d]
$L_{Mg:Mg,Y} = L_{Y:Mg,Y} = -21{,}000 + 7.5T$[d]

Laves-C15 (Cu_2Mg-type): (Ce, Mg, Mn, Y)$_2$ [Ce, Mg, Mn, Y]

G(Ce:Ce) = 3G(Ce,FCC-A1) + 62,760
G(Ce:Mg) = 2G(Ce,FCC-A1) + G(Mg,HCP-A3) + 41,840
G(Ce:Mn) = 2G(Ce,FCC-A1) + G(Mn,CBCC-A12) + 41,840
G(Ce:Y) = 2G(Ce,FCC-A1) + G(Y,HCP-A3) + 41,840
G(Mg:Ce) = 2G(Mg,HCP-A3) + G(Ce,FCC-A1)− 47,449 + 10.35T
G(Mg:Mg) = 3G(Mg,HCP-A3) + 15,000[b]
G(Mg:Mn) = 2G(Mg,HCP-A3) + G(Mn,CBCC-A12) + 49,340
G(Mg:Y) = 2G(Mg,HCP-A3) + G(Y,HCP) − 20,920
G(Mn:Ce) = 2G(Mn,CBCC-A12) + G(Ce,FCC-A1) + 41,840
G(Mn:Mg) = 2G(Mn,CBCC-A12) + G(Mg,HCP-A3) + 49,340
G(Mn:Mn) = 3G(Mn,CBCC-A12) + 83,680
G(Mn:Y) = 2G(Mn,CBCC-A12) + G(Y,HCP-A3) − 7,200 + 12.57T
G(Y:Ce) = 2G(Y,HCP-A3) + G(Ce,FCC-A1) + 41,840
G(Y:Mg) = 2G(Y,HCP-A3) + G(Mg,HCP) + 88,220
G(Y:Mn) = 2G(Y,HCP-A3) + G(Mn,CBCC-A12) + 174,560 − 12.57T
G(Y:Y) = 3G(Y,HCP-A3) + 125,520

BCC-B2 (CsCl-type): (Mg, Mn)[Ce, Mg, Y]

G(Mg:Ce) = G(Mg,HCP-A3) + G(Ce,FCC-A1) − 28,600 + 5.08T
G(Mg:Mg) = 2G(Mg,HCP-A3) + 8,368
G(Mg:Y) = G(Mg,HCP-A3) + G(Y,HCP-A3) − 29,031.03 + 6.06T
G(Mn:Ce) = G(Mn,CBCC-A12) + G(Ce,FCC) + 83,680
G(Mn:Mg) = G(Mn,CBCC-A12) + G(Mg,HCP-A3) + 41,840
G(Mn:Y) = G(Mn,CBCC-A12) + G(Y,HCP-A3) − 836.8

HCP-A3: (Ce, Mg, Mn, Y)

G(Ce,HCP-A3) = G(Ce,FCC-A1) + 5230
$L_{Ce,Mg}$ = −24,476.4
$L_{Ce,Mn}$ = 62,760
$L_{Ce,Y}$ = 0
$L_{Mg,Mn} = 37{,}148.1 - 1.8103T$[c]
$L_{Mg,Y} = -27{,}031.25 + 13.95T - 2{,}836.21(X_{Mg} - X_Y)$[d]
$L_{Mn,Y}$ = 62,760

BCC-A2: (Ce, Mg, Mn, Y)

$L_{Ce,Mg} = -15{,}594.01 - 9.75T + 9340.62(X_{Ce} - X_{Mg})$
$L_{Ce,Mn} = 35{,}982.4 + 4184(X_{Ce} - X_{Mn})$
$L_{Ce,Y}$ = 2092
$L_{Mg,Mn}$ = 83,680
$L_{Mg,Y} = -48{,}242.98 + 25.5T$
$L_{Mn,Y}$ = 62,760

FCC-A1: (Ce, Mg, Mn, Y)

$L_{Ce,Mg} = -9{,}273.15 - 2.07T$
$L_{Ce,Mn} = 41{,}840 + 6276(X_{Ce} - X_{Mn})$
$L_{Ce,Y}$ = 0
$L_{Mg,Mn}$ = 83,680
$L_{Mg,Y}$ = 62,760
$L_{Mn,Y}$ = 62,760

DHCP-A3′: (Ce, Y)

G(Ce) = G(Ce,FCC-A1) − 1,200 + 4.2T
G(Y) = G(Y,HCP-A3)(f) + 6,276
$L_{Ce,Y} = -8840.34 - 4.2T$

$Mg_{24}Y_5$: (Mg)$_{24}$[Mg, Y]$_4${Y}$_1$

G(Mg:Mg:Y) = 28G(Mg,HCP-A3) + G(Y,HCP-A3) − 21,170.12
G(Mg:Y:Y) = 24G(Mg,HCP-A3) + 5G(Y,HCP-A3) −227,282.29 + 36.53T[d]

Stoichiometric compounds

Compound	$H°_{298.15K}$, J/mol	$S°_{298.15K}$, J/mol · K	C_p, J/mol · K
$CeMg_{12}$	−139,880.0	377.01	$C_p = C_p$ (Ce,FCC-A1) + 12 × C_p (Mg,HCP-A3)
Ce_2Mg_{17}	−215,906.0	591.63	$C_p = 2 \times C_p$ (Ce,FCC-A1) + 17 × C_p (Mg,HCP-A3)
Ce_5Mg_{41}	−576,002.0	1387.78	$C_p = 5 \times C_p$ (Ce,FCC-A1) + 41 × C_p (Mg,HCP-A3)
$CeMg_3$	−76,000.0	140.97	$C_p = C_p$ (Ce,FCC-A1) + 3 × C_p (Mg,HCP-A3)
$Mn_{23}Y_6$	−153,700.0	1046.82	$C_p = 23 \times C_p$ (Mn,CBCC-A12) + 6 × C_p (Y,HCP-A3)
$Mn_{12}Y$	−32,695.9	440.59	$C_p = 12 \times C_p$ (Mn,CBCC-A12) + C_p (Y,HCP-A3)

(a) For all pure elements (Ce, Mg, Mn and Y). (b) Ref 78. (c) Ref 79. (d) Ref 68. (e) Ref 34. (f) G(Y,HCP-A3) from Ref 5

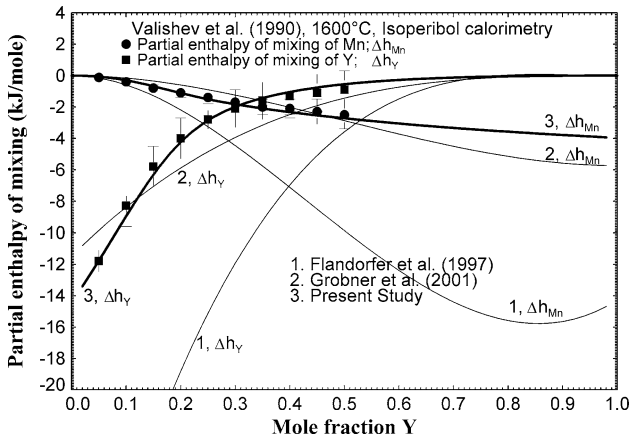

Fig. 1 Partial enthalpies of mixing of Mn and Y in liquid Mn-Y alloys at 1600°C. Comparison of experimental data with optimizations from present study and by Flandorfer et al.[16] and Gröbner et al.[17]. Data points from Valishev et al.[20]

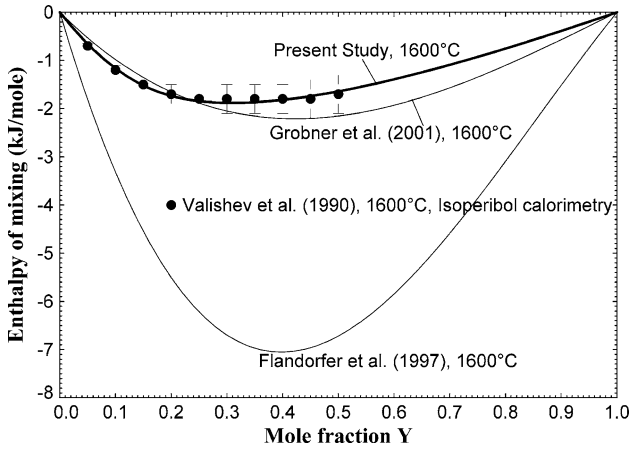

Fig. 2 Enthalpy of mixing[20] in liquid Mn-Y alloys at 1600°C. Comparison of experimental data with optimizations from present study and by Flandorfer et al[16] and Gröbner et al.[17]. Data points from Valishev et al.[20]

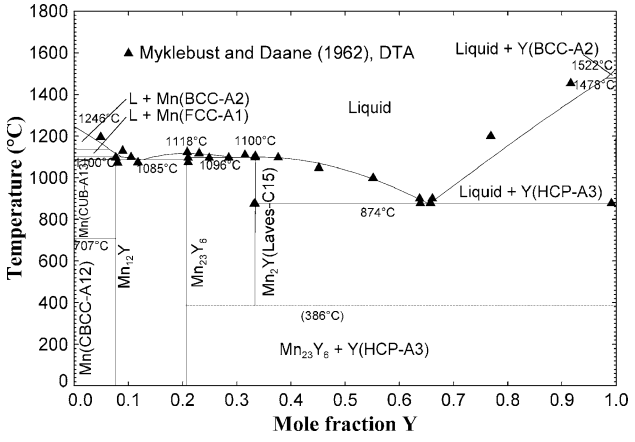

Fig. 3 Optimized phase diagram of the Mn-Y system. Closed triangles from Myklebust and Daane[18]

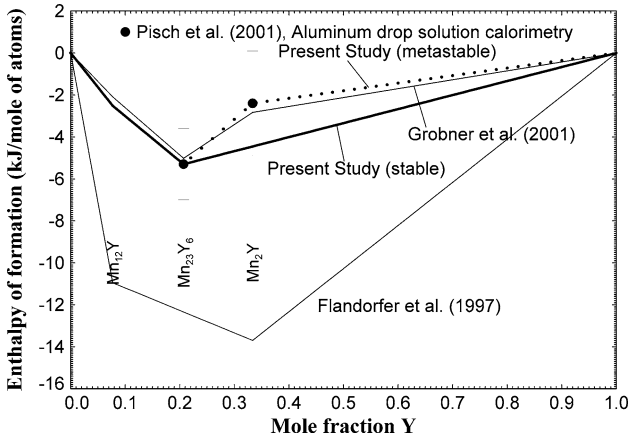

Fig. 4 Enthalpy of formation of intermetallic compounds in the Mn-Y system at 25°C. Dashed line is metastable enthalpy of formation (Mn_2Y is not stable at 25°C). From Flandorfer et al.,[16] Gröbner et al.,[17] and Pisch et al.[19]

the enthalpies of $Mn_{23}Y_6$ and Y(HCP). As a result, it is not stable at lower temperatures. As seen in Fig. 3, Mn_2Y is calculated to decompose to $Mn_{23}Y_6$ and Y below ~386°C when the optimized enthalpy of formation of Mn_2Y (−2.4 kJ/mole of atoms) is taken to be the same as the measured value.[19]

3.2 The Mg-Mn System

This system was extensively reviewed by Nayeb-Hashemi and Clark[22] and was optimized by Tibbals.[23] The system exhibits negligible solubility of Mg in solid Mn, very limited solubility of Mn in solid Mg and wide immiscibility in liquid alloys. No intermetallic compounds have been reported. Many investigations have been carried out to determine the solubility of Mn in both HCP and liquid Mg.[24-33] Recently, Gröbner et al.[34] measured the monotectic temperature by DTA using a sealed Ta crucible. Based on their measurements, they revised the previous thermodynamic description of Tibbals.[23]

Both previous optimizations[23,34] reproduce the observed solubilities of Mn in both HCP and liquid Mg, and the optimization by Gröbner et al. also reproduces the measured monotectic temperature.

The consolute temperature of the binary miscibility gap has not been measured. The earlier optimizations[23,34] calculate it at 4359 and 3202°C, respectively.

Antion[35] evaluated the Mg-Mn-Y ternary system and reported that such high binary consolute temperatures result in a calculated miscibility gap in the ternary system that is much larger than that observed experimentally. Hence, in the present study, we reoptimized the liquid in the Mg-Mn system with simultaneous consideration of the experimental data in the Mg-Mn-Y system. The resultant calculated binary consolute temperature is 1902°C. Figure 5 shows the

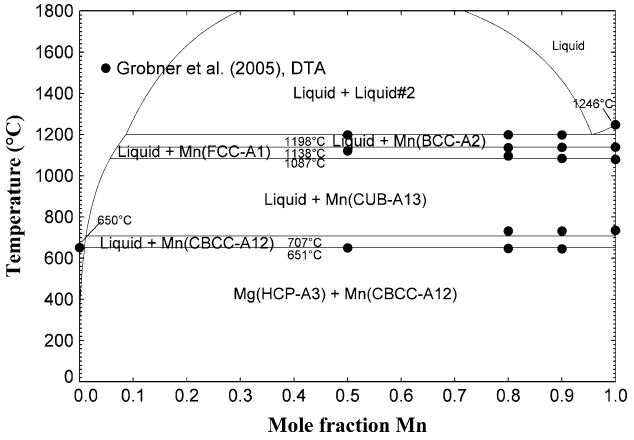

Fig. 5 Optimized phase diagram of the Mg-Mn system. Closed circle from Gröbner et al.[34]

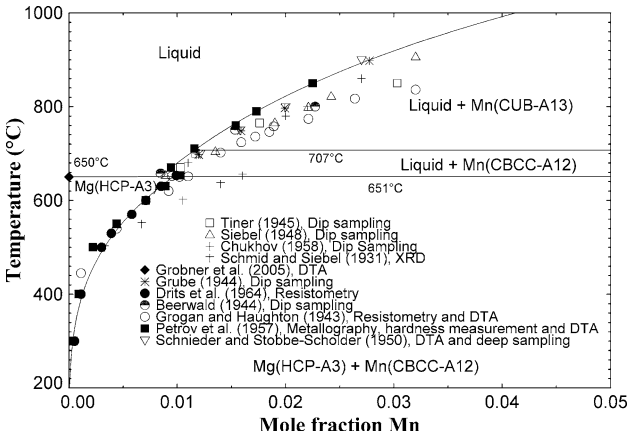

Fig. 6 Optimized phase diagram of the Mg-Mn system in the Mg-rich region. Data points from Schmid and Siebel,[24] Grogan and Haughton,[25] Beerwald,[26] Grube,[27] Tiner,[28] Siebel,[29] Schneider and Stobbe-Scholder,[30] Petrov et al.,[31] Chukhov,[32] Drits et al.,[33] and Gröbner et al.[34]

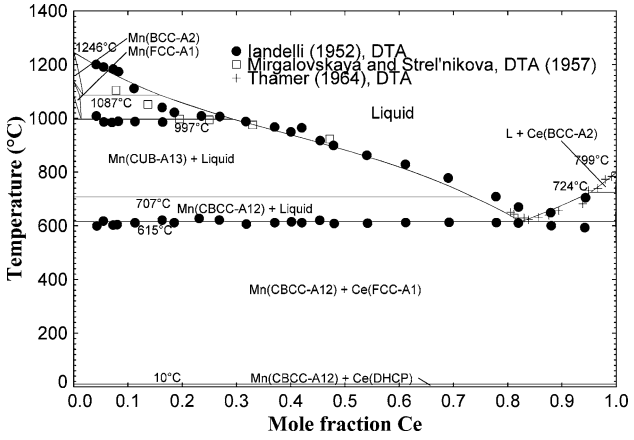

Fig. 7 Optimized phase diagram of the Ce-Mn system. Data points from Iandelli,[36] Mirgalovskaya and Strel'nikova,[37] and Thamer[38]

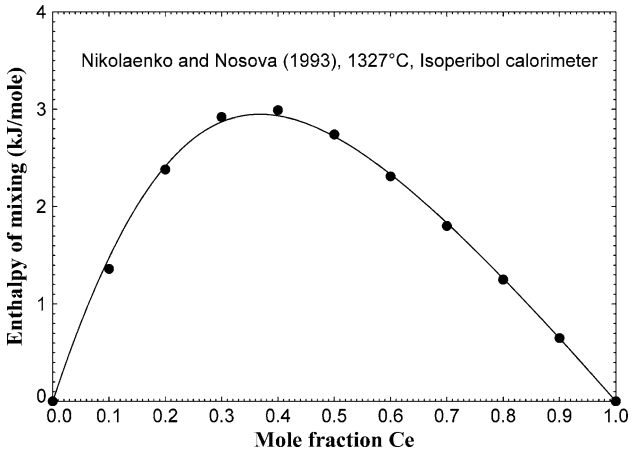

Fig. 8 Enthalpy of mixing in liquid Ce-Mn alloys at 1327°C. Comparison of experimental data (Nikolaenko and Nosova[39]) with optimizations from present study

present optimized phase diagram of the Mg-Mn system. Our subsequent optimization of the Mg-Mn-Y system[1] agrees well with the experimental data of Antion[35] without the need for any adjustable ternary parameters for the liquid phase. Calculated solubilities of Mn in both HCP and liquid Mg are shown in Fig. 6 along with the experimental data.

3.3 The Ce-Mn System

The phase diagram has been investigated by thermal analysis, and enthalpies of mixing of liquid Ce-Mn alloys have been reported. An early investigation employing thermal analysis by Iandelli[36] reported two thermal arrests at 612 and 998°C. The latter was interpreted as a monotectic temperature associated with a narrow miscibility gap.[36] In a later thermal analysis investigation, Mirgalovskaya and Strel'nikova,[37] reported the two temperatures 998 and 1087°C as allotropic transition temperatures accompanying a small solubility of Ce in Mn (FCC and BCC). This interpretation has been adopted in the present optimization. It is possible that hydrogen impurities in Mn could have given spurious results in the earlier study. Thamer examined the phase diagram in the Ce-rich region by differential thermal analysis (DTA), x-ray diffraction (XRD), and metallography.[38] According to Iandelli[36] and Thamer,[38] the solubility of Ce in Mn is virtually zero at room temperature and at 600°C. The solubility of Mn in Ce(FCC) is assumed to be negligible, there being no evidence to the contrary. Figure 7 shows the optimized phase diagram along with the experimental data.

Ce-Mn liquid alloys exhibit small positive enthalpies of mixing.[39]The calculated integral enthalpy of mixing at 1327 in Fig. 8 along with the experimental data. The entropy of mixing is close to ideal. Hence with $Z^{Mn}_{CeMn}/Z^{Ce}_{CeMn} = 1/2$, the MQM reduces nearly to a Bragg-Williams model with the excess Gibbs energy as a polynomial in the

equivalent fractions as described in section 2.1, giving the maximum in Fig. 8 near $X_{Ce} = 1/3$ as observed.

3.4 The Ce-Y System

Experimental information in the Ce-Y system is scarce. An earlier version of the phase diagram[40] showed complete miscibility at low temperatures between Ce(DHCP) and Y(HCP). Valletta[41] reported a δ phase (hexagonal αSm type) near 50 at.% Y, based probably on lattice parameter measurements. In a later investigation, Flandorfer et al.[42] studied the system by DTA. As well, they annealed samples at 500°C for 3000 h, followed by quenching and analysis by XRD. The δ phase was found to be metastable, and two-phase (FCC + DHCP) and (DHCP + HCP) regions were observed. The optimized phase diagram is shown in Fig. 9 along with the experimental points of Flandorfer et al.[42] The transformation temperature from pure FCC(Ce) to pure DHCP(Ce) was changed from 61°C (the current value in the COST-507 database[43]) to 10°C according to the recent investigation by Gschneidner et al.[44]

Flandorfer et al.[42] observed two phases (FCC + DHCP) at equilibrium at overall compositions of 10 and 25 at.% Y at 500°C as shown in Fig. 9. However, such a wide two-phase region is inconsistent with the measurements by Gschneidner et al.[44] who reported an enthalpy of transformation from DHCP(Ce) to FCC(Ce) of 181 ± 12 J/mol based on differential scanning calorimeter measurements. With such a small enthalpy of transformation, the thermodynamically calculated width of the two-phase region at 500°C is only a few atomic percent. Hence, we must reject either the measurements[44] of the enthalpy of transformation or the observation[42] of the relatively wide two-phase region. We have chosen the former option and have adjusted the enthalpy of transformation accordingly to 1200 J/mol to reproduce the phase diagram measurements. However, further experimental work is required to decide this point.

The Gibbs energy of hypothetical pure Ce(HCP) was optimized by simultaneous consideration of data for the Ce-Y and Ce-Mg systems to reproduce the measured relatively large solubility of Ce in Y(HCP) as shown in Fig. 9, and in Mg(HCP), as is discussed in section 3.5.

Flandorfer et al.[42] interpreted their DTA points near 780°C as indicating a peritectoid reaction at this temperature. In the present optimization, these points have been reinterpreted as shown in Fig. 9. Because of the paucity and scatter of the experimental data, and because of the aforementioned discrepancy between the enthalpy of transformation of Ce and the measured two-phase region, the optimized phase diagram should be regarded as tentative, pending future experimental investigations.

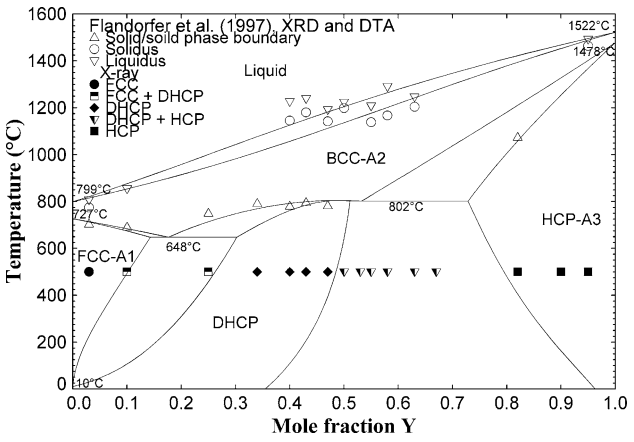

Fig. 9 Optimized phase diagram of the Ce-Y system. Source: Flandorfer et al.[42]

3.5 The Mg-Ce System

This system was extensively reviewed by Nayeb-Hashemi and Clark[45] and was thermodynamically optimized by Cacciamani et al.[46] The system has six intermetallic compounds. Ce_2Mg_{17} and $CeMg_2$ are stable only over limited temperature ranges. $CeMg_{12}$ has two polymorphs (body-centered orthorhombic and tetragonal), although the exact phase transformation temperature is not known. A $CeMg_{12}$(II) allotrope with a body-centered, totally ordered, orthorhombic structure (*oI*338, *Immm*) was first reported by Johnson et al.[47] from single-crystal XRD analyses. Later, however, its existence was rejected by Deportes et al.,[48] who did not observe higher-order harmonics that were expected from the structure suggested by Johnson et al.[47] In the present study, only tetragonal $CeMg_{12}$ was considered. The solubility of Ce in the HCP phase[49-54] and of Mg in theFCC phase[55,56] have been measured by several investigators.

The previous optimization by Cacciamani et al.[46] reproduces the phase diagram and thermodynamic properties of liquid alloys reasonably well. However, their calculated solubility of Ce in Mg(HCP) is virtually zero, contrary to the experimental data, because the value of the Gibbs energy for the hypothetical phase transformation of pure Ce from stable FCC to unstable HCP used by Cacciamani et al.[46] was very positive (50,000 J/mole). The use of this very positive value also makes it very difficult to reproduce the large solubility of Ce in Y(HCP) in the Ce-Y system (See section 3.4). Consequently, the Gibbs energy of the hypothetical phase transformation of pure Ce has been revised in the present study to 5230 J/mole by taking into account data for both the Mg-Ce and Ce-Y systems. This value is in reasonable agreement with the value of 8500 J/mole suggested by Wang et al.[57] from first-principles calculations at 0 K.

The liquid alloy was modeled with the MQM with maximum SRO at the composition $X_{Mg} = 3/4$ ($CeMg_3$) as evidenced by the fact that the enthalpy of mixing passes through a minimum near this composition (and also by the fact that the most stable solid compound is found at this composition). Figure 10 shows the calorimetrically measured integral enthalpy of mixing in liquid Mg-Ce alloys, along with optimized curves from the present study and from Cacciamani et al.[46] Figure 11 shows the calculated entropy of mixing in liquid Mg-Ce alloys. The "m" shape of the entropy of mixing in Fig. 11 results naturally in the MQM because the maximum in SRO occurs near $X_{Ce} = 1/4$,

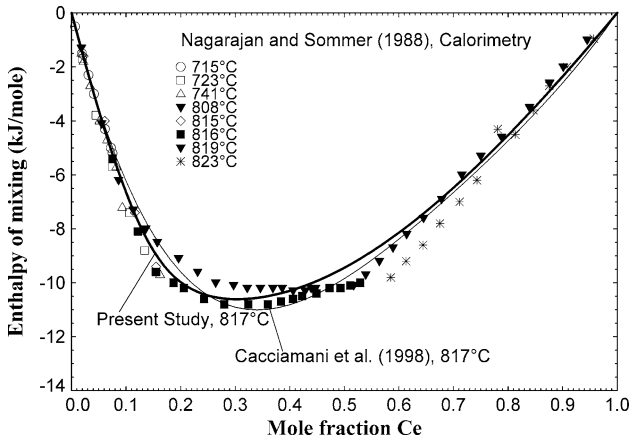

Fig. 10 Enthalpy of mixing in liquid Mg-Ce alloys at 817°C. Comparison of experimental data (Nagarajan and Sommer[63]) with optimizations from present study and by Cacciamani et al.[46]

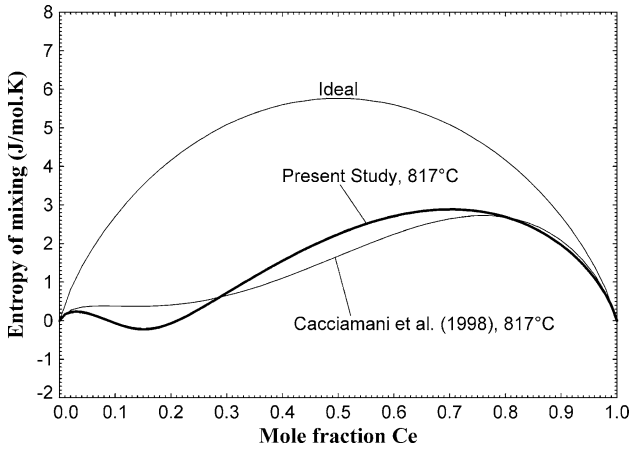

Fig. 11 Calculated entropy of mixing in liquid Mg-Ce alloys at 817°C. Comparison of experimental data with optimizations from present study and by Cacciamani et al.[46]

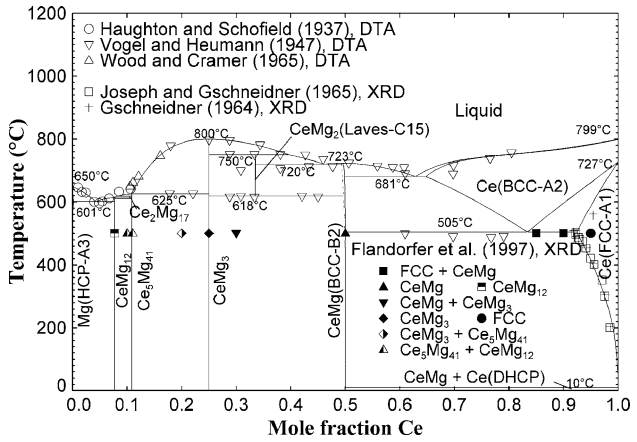

Fig. 12 Optimized phase diagram of the Mg-Ce system. Data points from Flandorfer et al.,[42] Haughton and Schofield,[49] Gschneidner,[55] Joseph and Gschneidner,[56] Vogel and Heumann,[58] and Wood and Cramer[59]

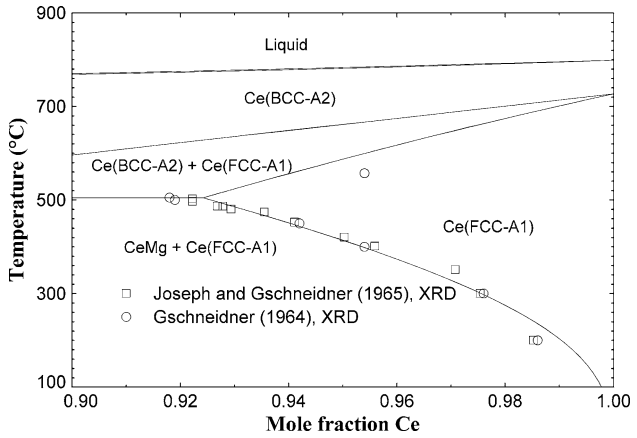

Fig. 13 Solubility of Mg in Ce(FCC). Comparison of experimental data (Gschneidner,[55] Joseph and Gschneidner[56]) with optimizations from present study

whereas with the Bragg-Williams model used by Cacciamani et al.,[46] it is necessary to introduce arbitrary excess entropy terms in order to reproduce this shape.

The optimized phase diagram of the Mg-Ce system is shown in Fig. 12 to 14 along with reported experimental data.[42,49,55,56,58,59] There is a large discrepancy in the Ce solubilities in the HCP phase as reported by different investigators. Rokhlin[54] used higher purity Mg than the other investigators, and Park and Wyman[52] annealed their samples for a longer time (~1000 h). These two investigations suggest a relatively low solubility of Ce in the HCP phase, and this was accepted in the present study. Solubilities of alloying elements in the HCP phase are of great practical importance, and it would be worthwhile to reinvestigate the solubilities in this region experimentally.

Figure 15 shows measured[60-63] and optimized enthalpies of formation of the intermetallic compounds. The optimized enthalpy of formation of CeMg in the present study is less negative than that of Cacciamani et al.[46] but close to recently measured experimental data.[62] Vapor pressure measurements of Mg over liquid alloys were conducted by Bayanov et al.,[64] and these are compared with the optimized thermodynamic calculations in Fig. 16. Although the calculations are slightly higher than the experimental vapor pressure data, the temperature dependence is in good agreement.

A small nonstoichiometry of the CeMg BCC-B2 phase at high temperature (see Fig. 12) is predicted based on the Henrian activity coefficient of Mg in this structure obtained from our optimizations of other MMg BCC-B2 phases. However, no measurements of the extent of this nonstoichiometry are available.

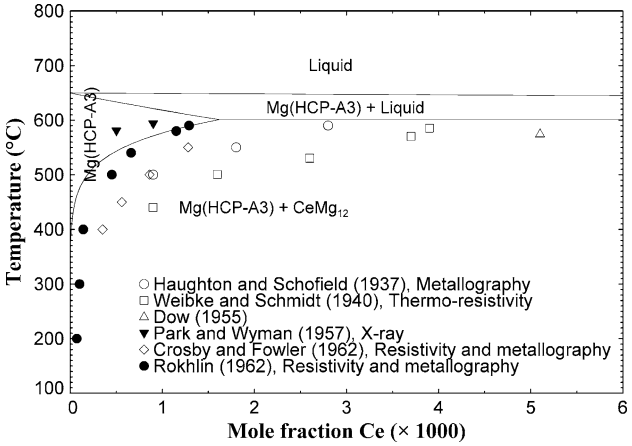

Fig. 14 Solubility of Ce in Mg(HCP). Comparison of experimental data with optimizations from present study. Data points from Haughton and Schofield,[49] Weibke and Schmidt,[50] Dow,[51] Park and Wyman,[52] Crosby and Fowler,[53] and Rokhlin[54]

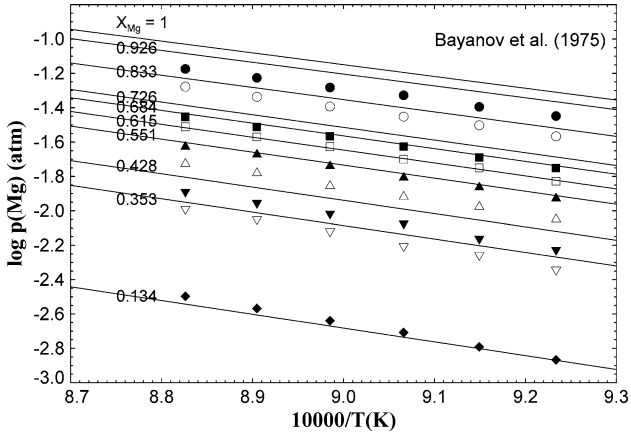

Fig. 16 Vapor pressure of Mg over liquid Mg-Ce alloys. Comparison of experimental data (Bayanov et al.[64]) with optimizations from present study. Numbers on lines are overall mole fraction of Mg in the liquid phase

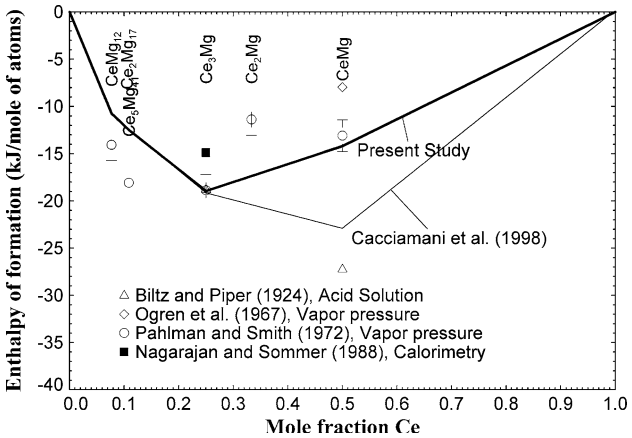

Fig. 15 Enthalpy of formation of intermetallic compounds in the Mg-Ce system at 25°C. Data points from Biltz and Piper,[60] Orgen et al.,[61] Pahlman and Smith,[62] and Nagarajan and Sommer[63]

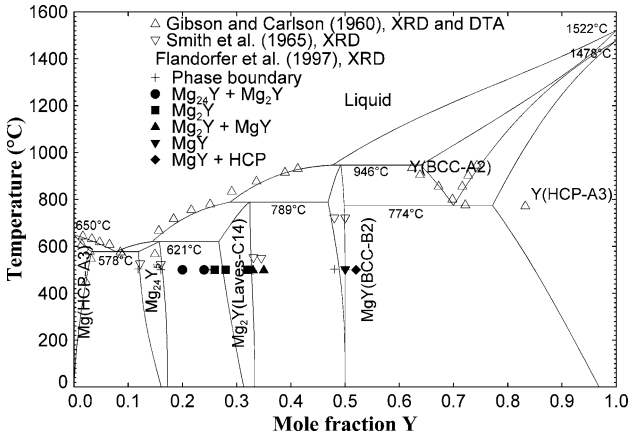

Fig. 17 Optimized phase diagram of the Mg-Y system. Data points from Flandorfer et al.,[42] Gibson and Carlson,[71] and Smith et al.[72]

3.6 The Mg-Y System

A thermodynamic optimization of the Mg-Y system was first carried out by Ran et al.,[65] who used the Wagner-Schottky model[66] to describe the nonstoichiometry of the $Mg_{24}Y_5$ and MgY phases. Later, Lukas[67] revised the optimization using different modeling for the solid solutions. The system has been reoptimized by Fabrichnaya et al.,[68] using more recent calorimetric data for the liquid alloys[69] and crystal structure data for the intermetallic phases,[42,70] modeling $Mg_{24}Y_5$, Mg_2Y (Laves-C14), and MgY (BCC-B2) using the CEF,[14] and treating MgY as an ordered BCC phase. Generally, this latest optimization by Fabrichnaya et al.[68] reproduces most of the experimental information well except for the phase boundary between HCP(Mg) and $Mg_{24}Y_5$. An accurate thermodynamic description of Mg-rich alloys and of solubilities in these alloys is of great importance. Furthermore, as discussed in section 1, the use of the MQM to account for SRO in liquid alloys will generally result in better predictions in ternary and higher-order systems. For these reasons, in the present study we have revised the optimization of Fabrichnaya et al.[68]

Figures 17 and 18 show the optimized phase diagram along with reported experimental data.[42,71-76] Model parameters of the $Mg_{24}Y_5$ phase were slightly changed from those of Fabrichnaya et al.[68] in order to reproduce the reported phase boundary with Mg(HCP) more accurately. Figure 19 shows calorimetric data[69] for the integral enthalpies of mixing in liquid alloys along with calculations from the present and earlier optimizations. In the present study, the MQM was used for the liquid with the composition for maximum ordering at $X_Y = 1/3$. Calculations

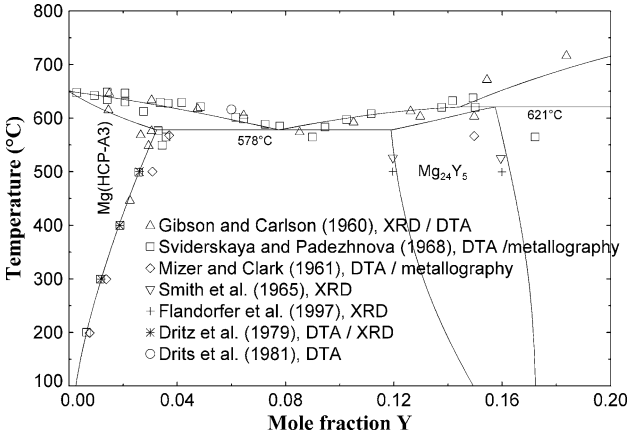

Fig. 18 Optimized phase diagram of the Mg-Y system in the Mg-rich region. Data points from Flandorfer et al.,[42] Gibson and Carlson,[71] Smith et al.,[72] Sviderskaya and Padezhnova,[73] Mizer and Clark,[74] and Drits et al.[75,76]

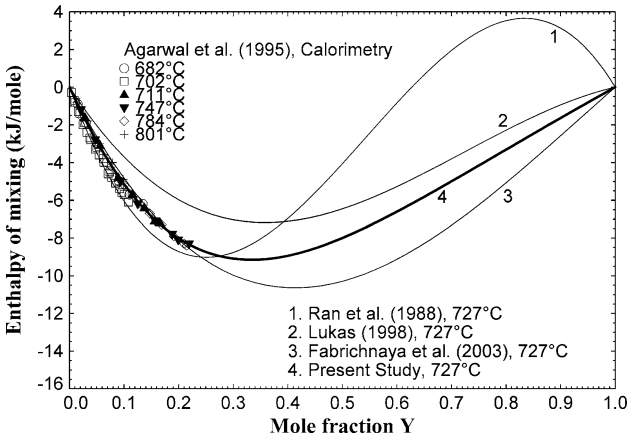

Fig. 19 Enthalpy of mixing in liquid Mg-Y alloys at 727°C. Comparison of experimental data (Agarwal et al.[69]) with optimizations from the present study and by Ran et al.,[65] Lukas,[67] and Fabrichnaya et al.[68]

from the present study and by Fabrichnaya et al.[68] are in good agreement with the experimental data, although the present optimization gives slightly superior fits in the Mg-rich region. The calculated entropy of mixing in liquid alloys is shown in Fig. 20. That of Fabrichnaya et al.[68] is almost flat, which seems unlikely, while that of Ran et al.[65] also seems unlikely. Figure 21 shows the calculated activity of Mg in liquid Mg-Y alloys at 900°C along with experimental data from vapor pressure measurements.[77]

Figure 22 compares enthalpies of formation at 25°C as measured by Smith et al.[72] employing differential acid solution calorimetry and the Knudsen effusion method with the optimized values in the present study. Also, the measured vapor pressures of Mg over Mg-Y alloys are in good agreement with calculations from the present study, as shown in Fig. 23.

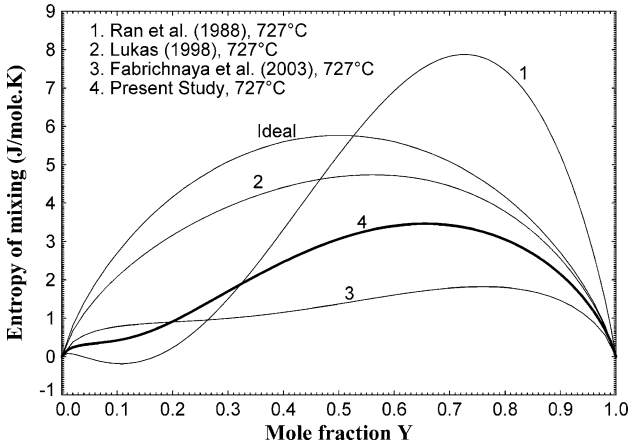

Fig. 20 Calculated entropy of mixing in liquid Mg-Y alloys at 727°C. Data points from by Ran et al.,[65] Lukas,[67] and Fabrichnaya et al.[68]

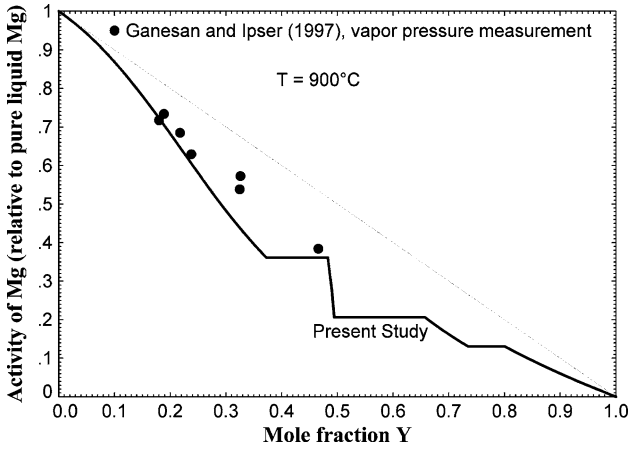

Fig. 21 Calculated activity of Mg (relative to pure liquid Mg) in Mg-Y alloys at 900°C. Data points from Ganesan and Ipser[77]

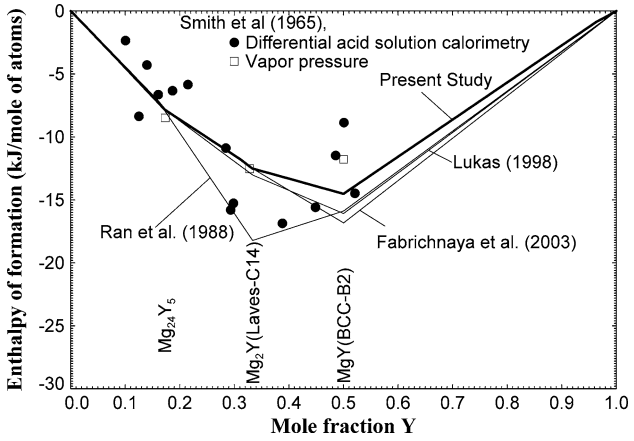

Fig. 22 Enthalpy of formation of intermetallic compounds in the Mg-Y system at 25°C. Data from Ran et al.,[65] Lukas,[67] Fabrichnaya et al.[68], and Smith et al.[72]

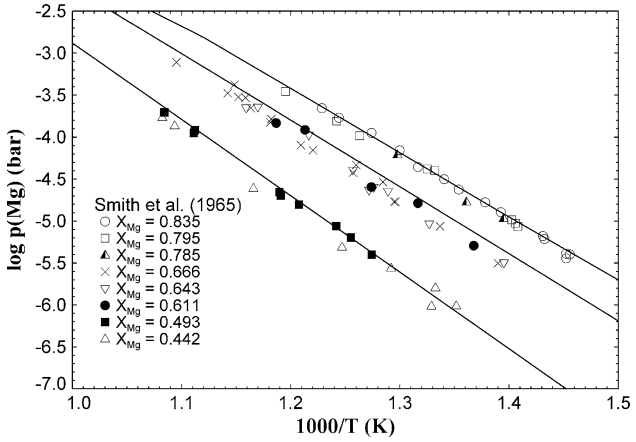

Fig. 23 Vapor pressures over Mg-Y alloy at several compositions. Comparison of experimental data with optimizations from present study. Data from Smith et al.[72]

4. Conclusions

A complete thermodynamic database has been prepared for all six binary subsystems of the Mg-Ce-Mn-Y system. All available thermodynamic and phase equilibrium data have been critically evaluated to obtain one set of optimized model parameters of the Gibbs energies of all phases that can reproduce the experimental data within experimental error limits. Evaluations/optimizations of the ternary subsystems have also been performed and will be reported in a subsequent article.[1]

The use of the Modified Quasi-chemical Model (MQM) for the liquid phase has permitted SRO to be taken into account. This provides better representations of the partial properties of solutes in solutions rich in Mg, the activities of solutes in dilute solution being of much practical importance. As will be shown in a forthcoming article, use of the MQM generally also results in better estimations of the properties of ternary and higher-order liquid alloys.

When the extent of SRO is small, the MQM reduces to a model in which the excess Gibbs energy is a polynomial expansion in the coordination-equivalent fractions rather than in the mole fraction. The composition of the maximum or minimum in the excess Gibbs energy curve can thereby be easily set to any desired value by fixing the ratio of the coordination numbers of the components. It has been shown that this method of setting the composition of the extremum can often represent the data better than the usual method of including subregular and higher polynomial terms in a Redlich-Kister expansion in the mole fractions, and again better representation of partial properties in dilute composition regions result.

Acknowledgment

Financial support from General Motors of Canada Ltd. and the Natural Sciences and Engineering Research Council of Canada through the CRD grant program is gratefully acknowledged. One of the author (YBK) wish to thank Dr. Alexander Pisch (LTPCM, Grenoble) for kindly providing unpublished data.

References

1. Y.-B. Kang, A.D. Pelton, P. Chartrand, P. Spencer, and C. Fuerst, Thermodynamic Database Development of the Mg-Ce-Mn-Y System for Mg Alloy Design, *Metall. Mater. Trans. A*, 2007, doi: 10.1007/s11661-007-9137-2
2. C.W. Bale, P. Chartrand, S.A. Degterov, G. Eriksson, K. Hack, R. Ben Mahfoud, J. Melançon, A.D. Pelton, and S. Petersen, FactSage Thermochemical Software and Databases, *Calphad*, 2002, **26**(2), p 189-228
3. C.W. Bale, A.D. Pelton, and W.T. Thompson, FactSage thermochemical software, http://www.factsage.com
4. A.T. Dinsdale, SGTE Data for Pure Elements, *Calphad*, 1991, **15**(4), p 317-425
5. A.T. Dinsdale, SGTE Data for Pure Elements, *Calphad*, 1991, **15**(4), p 317-425 plus updates (private communication), 2000, http://www.sgte.org
6. A.D. Pelton, S.A. Degterov, G. Eriksson, C. Robelin, and Y. Dessureault, The Modified Quasichemical Model I-Binary Solutions, *Metall. Mater. Trans. B*, 2000, **31B**(6), p 651-659
7. P. Chartrand and A.D. Pelton, Thermodynamic Evaluation and Optimization of the LiCl-NaCl-KCl-RbCl-CsCl-$MgCl_2$-$CaCl_2$ System Using the Modified Quasi-chemical Model, *Metall. Mater. Trans. A*, 2001, **32A**(6), p 1361-1383
8. P. Chartrand and A.D. Pelton, Thermodynamic Evaluation and Optimization of the LiF-NaF-KF-MgF_2-CaF_2 System Using the Modified Quasi-chemical Model, *Metall. Mater. Trans. A*, 2001, **32**(6), p 1385-1396
9. P. Chartrand and A.D. Pelton, Thermodynamic Evaluation and Optimization of the Li, Na, K, Mg, Ca//F, Cl Reciprocal System Using the Modified Quasi-chemical Model, *Metall. Mater. Trans. A*, 2001, **32A**(6), p 1417-1430
10. S.A. Decterov, I.-H. Jung, E. Jak, Y.-B. Kang, P. Hayes, and A.D. Pelton, Thermodynamic Modelling of the Al_2O_3-CaO-CoO-CrO-Cr_2O_3-FeO-Fe_2O_3-MgO-MnO-NiO-SiO_2-S System and Application in Ferrous Process Metallurgy, *VII International Conference on Molten Slags, Fluxes and Salts*, C. Pistorius, Ed., Jan 25-28 (Cape Town), The South African Institute of Mining and Metallurgy, Johannesburg, Rep. of South Africa, 2004, p 839-850
11. P. Waldner and A.D. Pelton, Thermodynamic Modeling of the Ni-S System, *Z. Metallkd.*, 2004, **95**, p 672-681
12. P. Waldner and A.D. Pelton, Critical Thermodynamic Assessment and Modeling of the Fe-Ni-S System, *Metall. Mater. Trans. B*, 2004, **35**(5), p 897-907
13. P. Waldner and A.D. Pelton, Thermodynamic Modeling of the Fe-S System, *J. Phase Equilib. Diffus.*, 2005, **26**(1), p 23-38
14. M. Hillert, The Compound Energy Formalism, *J. Alloys Compd.*, 2001, **320**, p 161-176
15. A. Palenzona and S. Cirafici, The Mn-Y (Manganese-Yttrium) System, *J. Phase Equilib.*, 1991, **12**(4), p 474-478
16. H. Flandorfer, J. Gröbner, A. Stamou, N. Hassiotis, A. Saccone, P. Rogl, R. Wouters, H. Seifert, D. Maccio, R. Ferro, G. Haidemenopoulos, L. Delaey, and G. Effenberg, Experimental Investigation and Thermodynamic Calculation of the Ternary System Mn-Y-Zr, *Z. Metallkd.*, 1997, **88**(7), p 529-538
17. J. Gröbner, A. Pisch, and R. Schmid-Fetzer, Thermodynamic Optimization of the Systems Mn-Gd and Mn-Y Using New Experimental Results, *J. Alloys Compd.*, 2001, **317-318**, p 433-437

18. R.L. Myklebust and A.H. Daane, The Yttrium-Manganese System, *Trans. Metal. Soc. AIME*, 1962, **224**, p 354-357
19. A. Pisch, F. Hodaj, P. Chaudouet, and C. Colinet, Standard Enthalpies of Formation of Some Mn-Y and Mn-Sc Intermetallic Compounds, *J. Alloys Compd.*, 2001, **319**, p 210-213
20. M.G. Valishev, O.Yu. Sidorov, S.P. Kolesnikov, Yu.O. Esin, and A.Ya. Dubrovskii, Partial and Integral Heats of Mixing of Components in Manganese-Yttrium Molten Binary Alloys, *Rasplavy*, 1990, **6**, p 90-91, in Russian
21. A.D. Pelton, Calculation of a Binary Solidus from the Liquidus and Minimal Additional Thermodynamic Information, *Ber. Bunsenges. Phys. Chem.*, 1980, **84**, p 212-218
22. A.A. Nayeb-Hashemi and J.B. Clark, The Mg-Mn (Magnesium-Manganese) System, *Bull. Alloy Phase Diagrams*, 1985, **6**(2), p 160-164
23. J. Tibbals, Mg-Mn System, *COST 507-Thermochemical Databases for Light Metal Alloys*, I. Ansara, A.T. Dinsdale, and M.H. Rand, Ed., Vol 2, EUR 18499, 1998, p 215-217
24. E. Schmid and G. Siebel, Determination of Solid Solubility of Mn in Mg by X-ray Analysis, *Metallwirtschaft*, 1931, **10**(49), p 923-925, in German
25. J.D. Grogan and J.L. Haughton, Alloys of Magnesium, *Part XIV-The Constitution of the Magnesium-Rich Alloys of Magnesium and Manganese. J. Inst. Met.*, 1943, **69**, p 241-248
26. A. Beerwald, On the Solubility of Iron and Manganese in Magnesium and Magnesium-Aluminum Alloys, *Metallwirtschaft*, 1944, **23**, p 404-407, in German
27. G. Grube, Magnesium-Manganese Phase Diagram, 1944, quoted in Ref 26
28. N. Tiner, The Solubility of Manganese in Liquid Magnesium, *Trans. Met. Soc. AIME*, 1945, **161**, p 351-359
29. G. Siebel, The Solubility of Iron, Manganese, and Zirconium in Magnesium Alloys, *Z. Metallkd.*, 1948, **39**, p 22-27, in German
30. A. Schneider and H. Stobbe-Scholder, The Structure and Technical Preparation of Corrosion-Resistant Magnesium-Manganese Alloys, *Metall*, 1950, **4**(9/10), p 178-183
31. D.A. Petrov, M.S. Mirgalovskaya, I.A. Strelnikova, and E.M. Komova, The Constitution Diagram for the Magnesium-Manganese System, *Trans. Inst. Met. A.A. Baikova, Akad. Nauk SSSR*, 1957, **1**, p 142-143, in Russian
32. M.V. Chukhov, On the Solubility of Mn in Liquid Mg, *Legkie Splaavy, Akad. Nauk SSSR, Inst. Met. A.A. Baikova*, 1958, **1**, p 302-305, in Russian
33. M.E. Drits, Z.A. Sviderskaya, and L.L. Rokhlin, Solid Solubility of Mn in Mg, *Izv. Nauka, Moscow*, 1964, p 272-278, in Russian
34. J. Gröbner, D. Mirkovic, M. Ohno, and R. Schmid-Fetzer, Experimental Investigation and Thermodynamic Calculation of Binary Mg-Mn Phase Equilibria, *J. Phase Equilib. Diffus.*, 2005, **26**(3), p 234-239
35. C. Antion, Etude du système Mg-Mn-Y-Gd et Dévelopment d'Alliages de Magnésium pour des Applications Structurales a Chaud, *These Docteur de L'INPG*, Institut National Polytechnique de Grenoble, 2003, in French
36. A. Iandelli, Alloys from Cerium and Manganese, *Atti Accad. Nazl. Lincei, Rend.*, 1952, **13**, p 265-268
37. M.S. Mirgalovskaya and I.A. Strel'nikova, System Manganese-Cerium, *Akad. Nauk SSSR*, 1957, p 135-138, in Russian
38. B.J. Thamer, The System Cerium-Manganese in the Range of 0-20 Atomic per cent Manganese, *J. Less-Common Met.*, 1964, **7**, p 341-346
39. I.V. Nikolaenko and V.V. Nosova, Heats of Mixing of Manganese with Lanthanum, Cerium, and Praseodymium, *Rasplavy*, 1993, **1**, p 76-79, in Russian
40. K.A. Gschneidner and F.W. Calderwood, *Binary Alloy Phase Diagrams*, 2nd ed., ASM International, 1990, p 1130-1131
41. R.M. Valletta, Structures and Phase Equilibriums of Binary Rare Earth Metal Systems, Ph.D. Thesis, Iowa State University, 1960
42. H. Flandorfer, M. Giovannini, A. Saccone, P. Rogl, and R. Ferro, The Ce-Mg-Y System, *Metall. Mater. Trans. A*, 1997, **28**, p 265-276
43. I. Ansara, A.T. Dinsdale and M.H. Rand, *COST 507-Thermochemical Databases for Light Metal Alloys*, I. Ansara, A.T. Dinsdale, and M.H. Rand, Ed., Vol 2, EUR 18499, 1998, p 374
44. K.A. Gschneidner Jr., V.K. Pecharsky, J. Cho, and S.W. Martin, The β to γ Transformation in Cerium-A Twenty Year Study, *Scr. Mater.*, 1996, **34**(11), p 1717-1722
45. A.A. Nayeb-Hashemi and J.B. Clark, The Ce-Mg (Cerium-Magnesium) System, *Bull. Alloy Phase Diagrams*, 1988, **9**(2), p 162-172
46. G. Cacciamani, A. Saccone, and R. Ferro, Ce-Mg System, *COST 507-Thermochemical Databases for Light Metal Alloys*, I. Ansara, A.T. Dinsdale, and M.H. Rand, Ed., Vol 2, EUR 18499, 1998, p 137-140
47. Q.C. Johnson, G.S. Smith, D.H. Wood, and E.M. Cramer, A New Structure in the Magnesium-Rich Region of the Cerium-Magnesium System, *Nature*, 1964, **201**(8), p 600
48. J. Deportes, D. Givord, R. Lemaire, and H. Nagai, Long Period Super-Lattices due to Ordering of Pairs of Substitution Atoms in RM_5 Haucke Phases, *J. Less Common Met.*, 1975, **40**, p 299-304
49. J.L. Haughton and T.H. Schofield, Alloys of Magnesium, *Part V.-The Constitution of the Magnesium Rich Alloys of Magnesium and Cerium. J. Inst. Met.*, 1937, **60**, p 339-344
50. F. Weibke and W. Schmidt, On the Solubility of Lanthanides in Al, Mg and Homogeneous Alloys of Mg and Al, *Z. Electrochem.*, 1940, **46**, p 357-364, in German
51. Dow Chemical Company, Contract DA-11-022-ORD-1645, Project TB4-15, Summary report, Part I, 1955, quoted in Ref 45
52. J.J. Park and L.L. Wyman, Phase Relationships in Magnesium Alloys, *WACD Tech. Rep.*, 1957, **57-504**, p 33
53. R.L. Crosby and K.A. Fowler, Studies of Magnesium Alloys for Use at Moderate Temperatures, *U.S. Bur. Mines, Rep. Invest*., 1962, No. 6078, p 28
54. L.L. Rokhlin, Solid Solubility of Neodymium and Cerium in Solid State Magnesium, *Izv. Akad. Nauk SSSR, Otd. Tekh. Nauk, Met. Toplivo*, 1962, **2**, p 126-130, in Russian
55. K.A. Gschneidner Jr., Rare Earth Research II, *Proc. Third Conf.*, K.S. Vorres, Ed., Gordon and Breach Science Publishers, New York, 1964
56. R.R. Joseph and K.A. Gschneidner Jr., Solid Solubility of Magnesium in Some Lanthanide Metals, *Trans. Metall. Soc. AIME*, 1965, **233**, p 2063-2069
57. Y. Wang, S. Curtarolo, C. Jiang, R. Arroyave, T. Wang, G. Ceder, L.-Q. Chen, and Z.-K. Liu, Ab Initio Lattice Stability in Comparison with CALPHAD Lattice Stability, *Calphad*, 2004, **28**(1), p 79-90
58. R. Vogel and T. Heumann, Determination of Ce-Mg and La-Mg Systems, *Z. Metallkd.*, 1947, **38**, p 1-8, in German
59. D.H. Wood and E.M. Cramer, Phase Relations in the Magnesium Rich Portion of the Cerium-Magnesium System, *J. Less-Common Met.*, 1965, **9**, p 321-337
60. W. Biltz and H. Piper, On the Heat of Formation of Intermetallic Compounds, Cerium Alloys, *Z. Anorg. Chem.*, 1924, **134**, p 13-24, in German
61. J.R. Orgen, N.J. Magnani, and J.F. Smith, Thermodynamics of Formation of Binary Rare Earth-Magnesium Phases with CsCl-Type Structures, *Trans. Metall. Soc. AIME*, 1967, **239**, p 766-771

62. J.E. Pahlman and J.F. Smith, Thermodynamics of Formation of Compounds in Ce-Mg, Nd-Mg, Gd-Mg, Dy-Mg, Er-Mg and Lu-Mg Binary Systems in the Temperature Rage 650-930°K, *Metall. Trans.*, 1972, **3**, p 2423-2432
63. K. Nagarajan and F. Sommer, Calorimetric Investigations of Ce-Mg Liquid Alloys, *J. Less-Common Met.*, 1988, **142**, p 319-328
64. A.P. Bayanov, Yu.A. Frolov, and Yu.A. Afanas'yev, Determination of the Thermodynamic Properties of Ce-Mg Melts, *Izv. Akad. Nauk SSSR, Metally*, 1975, **3**, p 91-95, in Russian
65. Q. Ran, H.L. Lukas, G. Effenberg, and G. Petzow, Thermodynamic Optimization of the Mg-Y System, *Calphad*, 1988, **12**(4), p 375-381
66. C. Wagner and W. Schottky, Theory of Arranged Mixed Phases, *Z. Physik. Chem.*, 1930, **11**, p 163-210
67. H.L. Lukas, Mg-Y System, *COST 507-Thermochemical Databases for Light Metal Alloys*, I. Ansara, A.T. Dinsdale, and M.H. Rand, Ed., Vol 2, EUR 18499, 1998, p 224-226
68. O.B. Fabrichnaya, H.L. Lukas, G. Effenberg, and F. Aldinger, Thermodynamic Optimization in the Mg-Y System, *Intermetallics*, 2003, **11**, p 1183-1188
69. R. Agarwal, H. Feufel, and F. Sommer, Calorimetric Measurements of Liquid La-Mg, Mg-Yb and Mg-Y Alloys, *J. Alloys Compd.*, 1995, **217**, p 59-64
70. F. Bonhomme and K. Yvon, Synthesis and Crystal Structure Refinement of Cubic $Mg_{6.8}Y$, J, *Alloys Compd.*,, 1996, **232**, p 271-273
71. E.D. Gibson and O.N. Carlson, The Yttrium-Magnesium Alloy System, *Trans. ASM*, 1960, **52**, p 1084-1096
72. J.F. Smith, D.M. Bailey, D.B. Novotny, and J.E. Davison, Thermodynamics of Formation of Yttrium-Magnesium Intermediate Phases, *Acta Metall.*, 1965, **13**, p 889-895
73. Z.A. Sviderskaya and E.M. Padezhnova, Phase Equilibria in Mg-Y and Mg-Y-Mn Systems, *Izv. Akad. Nauk SSSR, Met.*, 1968, **6**, p 183-190, in Russian; TR: *Russ. Metall.*, 1968, **6**, p 126-130
74. D. Mizer and J.B. Clark, The Magnesium-Rich Region of the Magnesium-Yttrium Phase Diagram, *Trans. Met. Soc. AIME*, 1961, **221**, p 207
75. M.E. Drits, E.M. Padezhnova, and T.V. Dobatkina, Phase Equilibria in Mg-Y-Al Alloys, *Russ. Metall.*, 1979, **3**, p 197-201
76. M.E. Drits, E.M. Padezhnova, T.V. Dobatkina, and E.A. Voytekhova, The Magnesium Corner of the Mg-Y-Ce System, *Russ. Metall.*, 1981, **6**, p 200-203
77. V. Ganesan and H. Ipser, Thermodynamic Properties of Liquid Magnesium-Yttrium Alloys, *J. Chim. Phys.*, 1997, **94**(5), p 986-991
78. H.L. Lukas, Al-Mg System, *COST 507-Thermochemical Databases for Light Metal Alloys*, I. Ansara, A.T. Dinsdale, and M.H. Rand, Ed., Vol 2, EUR 18499, 1998, p 48-53
79. N. Saunders, Mn-Ti System, *COST 507-Thermochemical Databases for Light Metal Alloys*, I. Ansara, A.T. Dinsdale, and M.H. Rand, Ed., Vol 2, EUR 18499, 1998, p 241-244